eLIFE elifesciences.org

RESEARCH ARTICLE

Figures and figure supplements

Experience shapes activity dynamics and stimulus coding of VIP inhibitory cells

Marina Garrett *et al*

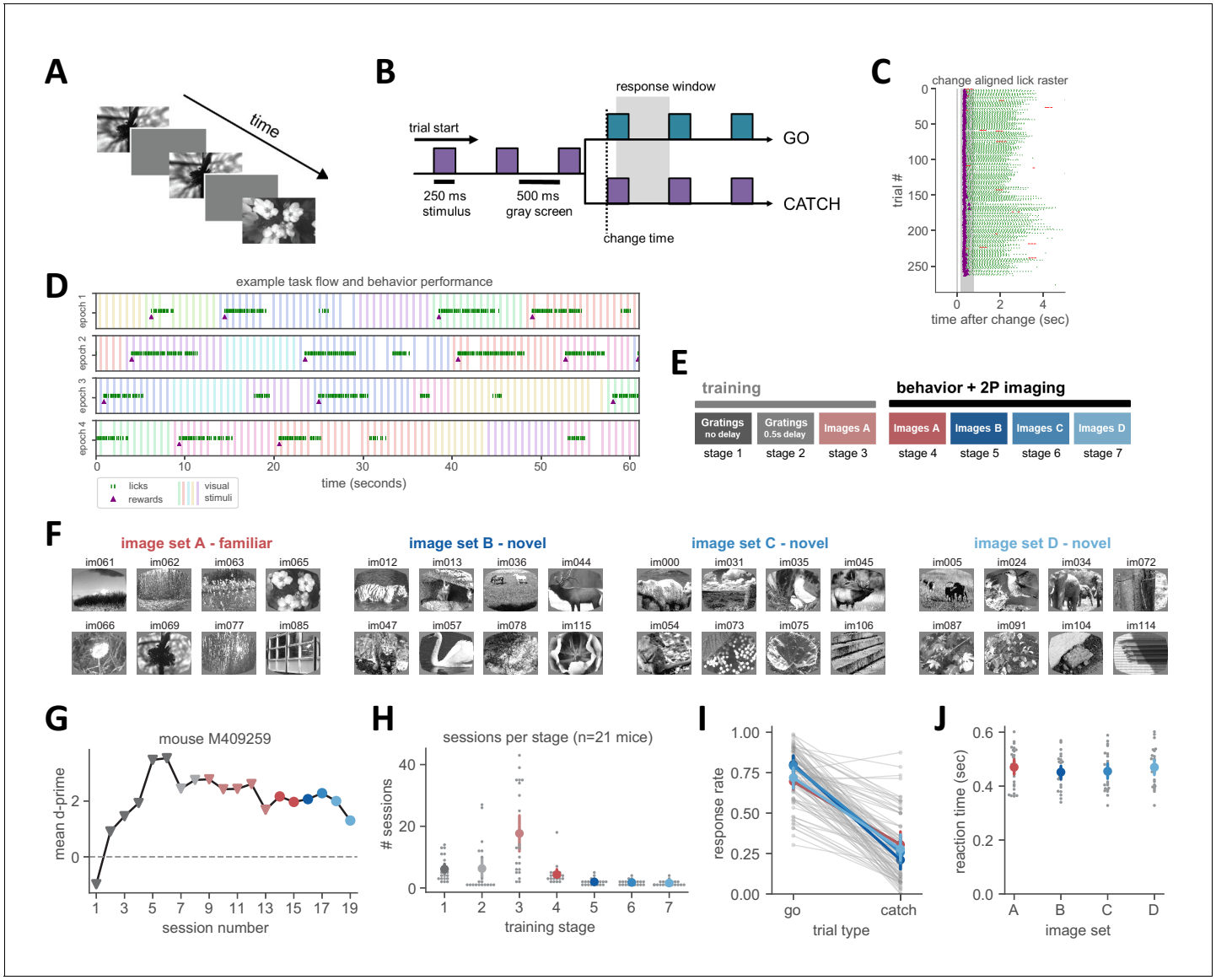

Figure 1. Natural image change detection task with familiar and novel images. (**A**) Schematic of stimulus presentation during the task. Images are presented for 250 ms followed by 500 ms of gray screen. (**B**) Trial structure. Colors represent different images. On go trials, the image identity changes and mice must lick within the 750 ms response window to receive a water reward. On catch trials no image change occurs and the behavioral response is measured to quantify guessing behavior. (**C**) Example lick raster, aligned to the image change time. Purple dots indicate rewards and green ticks are reward consumption licks. Red ticks indicate incorrect licking responses outside the response window. (**D**) Example behavior performance over four minutes of one session, separated into one-minute epochs. Colored vertical bars indicate stimulus presentations (different colors are different images). Green tick marks indicate licks, purple triangles indicate rewards. 5% of all non-change image flashes are omitted, visible as a gap in the otherwise regular stimulus sequence. (**E**) Training stages. Mice are initially trained with gratings of 2 orientations, first with no intervening gray screen (stage 1), then with a 500 ms inter-stimulus delay (stage 2). Next, mice perform change detection with eight natural scene images (stage 3, image set A). During the 2-photon imaging portion of the experiment, mice are tested with image set A as well as three novel image sets (B, C, D) on subsequent days. (**F**) The four sets of 8 natural images. Image set A is the familiar training set, and image sets B, C and D were the novel sets shown for the first time during 2-photon imaging. (**G**) Example training time course of one mouse. (**H**) Number of sessions spent in each stage across mice. Mean ± 95% confidence intervals in color, individual mice in gray. (**I**) Response rates for go and catch trials are similar across image sets. Individual behavior sessions are shown in gray and average ± 95% confidence intervals across sessions for each image set are shown in color. (J) Reaction times, measured as latency to first lick, are not significantly different across image sets. Mean ± 95% confidence intervals in color, individual sessions in gray.

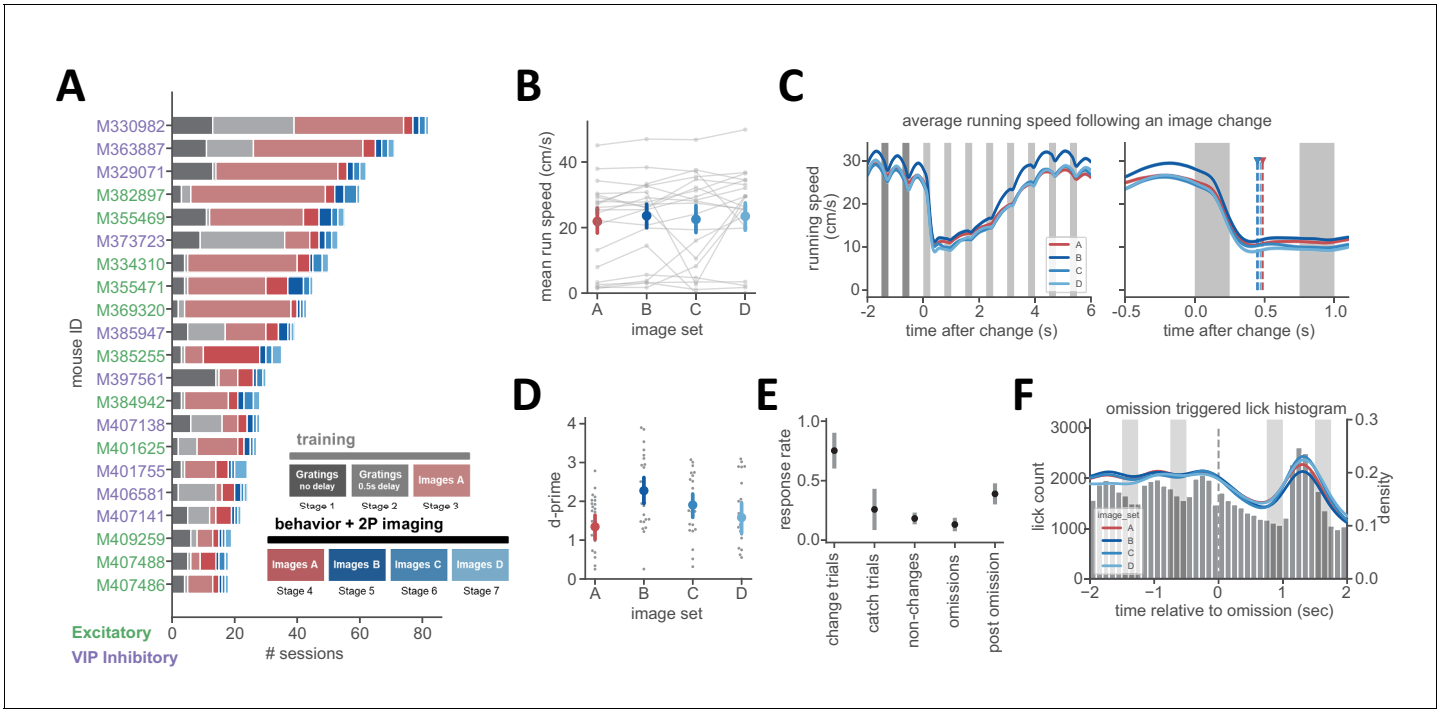

Figure 1—figure supplement 1. Behavior is similar across image sets. (**A**) Number of sessions in each training stage for all mice in the study. Slc17a7+ mice are shown in green and VIP+ mice are shown in purple. Inset shows color legend for training stages. (**B**) Average running speed is similar across image sets ($p>0.05$ for all image set comparisons, Welch's t-test used for all statistical comparisons, see Materials and methods for additional details). Mean running speed is computed for each stimulus presentation within a session then averaged across the session. Gray lines indicate session average running speed for each mouse, colors indicate average across mice with 95% confidence intervals. (**C**) Average change triggered running speed is similar across image sets. Right panel shows slowing of running behavior following a stimulus change, with median lick latency (values from ***Figure 1J***) for each image set indicated by arrows and dotted lines. (**D**) Mean d-prime is similar across image sets ($p>0.05$ for all image set pairs except A-B, where $p=0.002$). (**E**) Average licking response rate (± SEM) measured for image change trials, catch trials, all non-change stimulus presentations, stimulus omissions, and for the stimulus presentation immediately following an omitted stimulus. (**F**) Pattern of mouse licking behavior around the time of stimulus omission is similar across image sets. Gray bars show histogram of lick counts in each time bin pooled over all mice (left y-axis). Colored lines show kernel density estimate of lick distribution over time for each image set (right y-axis).

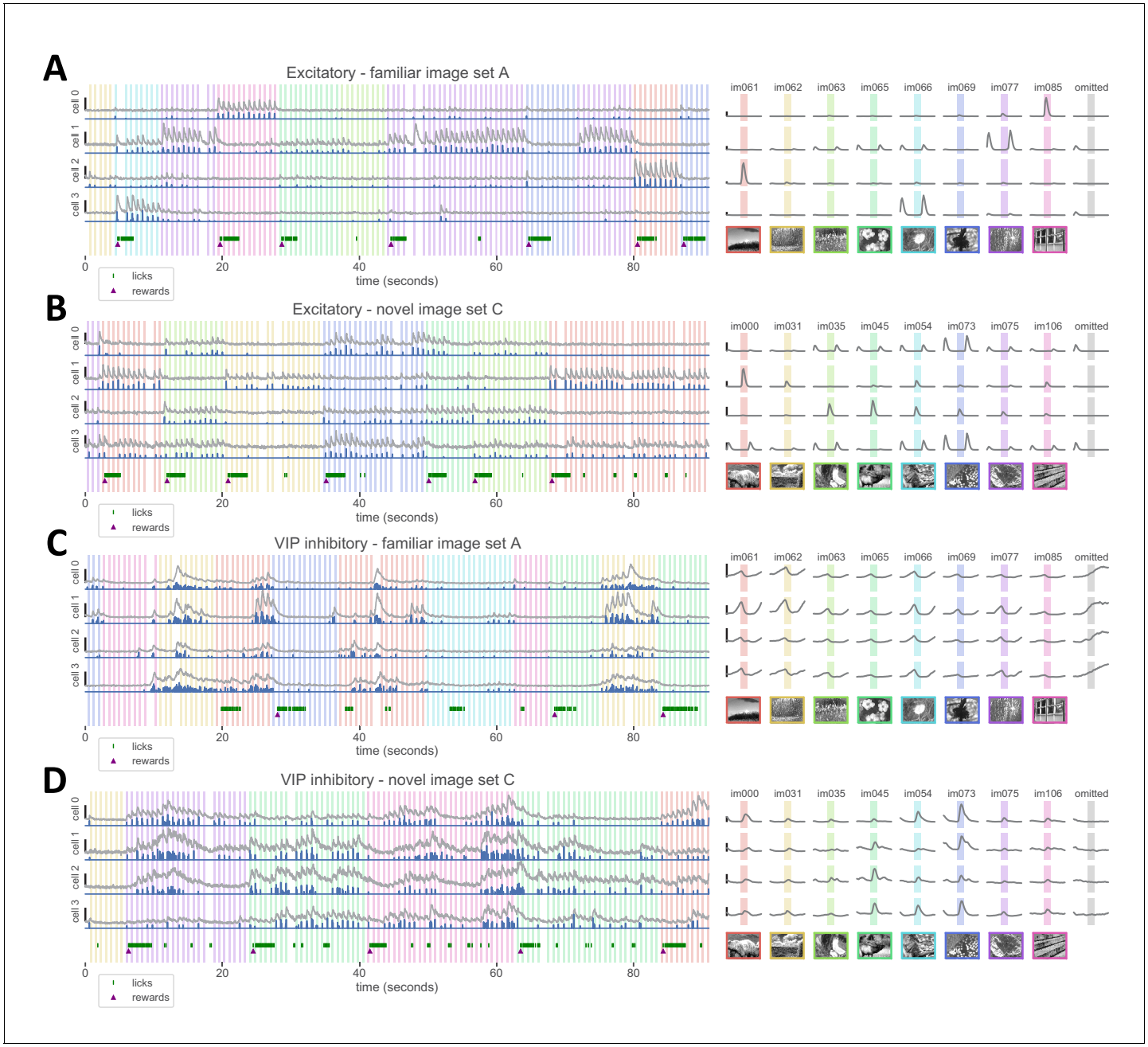

Figure 2. Activity in layer 2/3 excitatory and VIP inhibitory cells during change detection task. (**A**) Example cell responses to the familiar image set A, from excitatory cells in layer 2/3 of an Slc17a7-IRES2-Cre;CaMkII-tTa;Ai93 mouse expressing GCaMP6f. Left panel: dF/F traces (gray) from four excitatory cells over a 90 second epoch of a behavior session (scale bars on left indicate 75% dF/F). Deconvolved events are shown in blue below the dF/F trace. Colored vertical bars indicate image presentation times; timing of licks and reward delivery are shown at bottom. Right panel: response of the same 4 cells to each image, as well activity during stimulus omission (right column, gray shading indicates the time where a stimulus would have been displayed). Scale bars indicate 0.05 event magnitude in arbitrary units. (**B**) Example excitatory cells from a session with novel image set C. Left panel scale bars indicate 100% dF/F, right panel scale bars indicate event magnitude of 0.05. (**C**) Example VIP inhibitory cells from layer 2/3 of a VIP-IRES-Cre;Ai148 mouse expressing GCaMP6f, from a session with familiar image set A. Left panel scale bars indicate 225% dF/F, right panel scale bars indicate event magnitude of 0.05. (**D**) Example VIP inhibitory cells for a session with novel image set C. Left panel scale bars indicate 200% dF/F, right panel scale bars indicate event magnitude of 0.05.

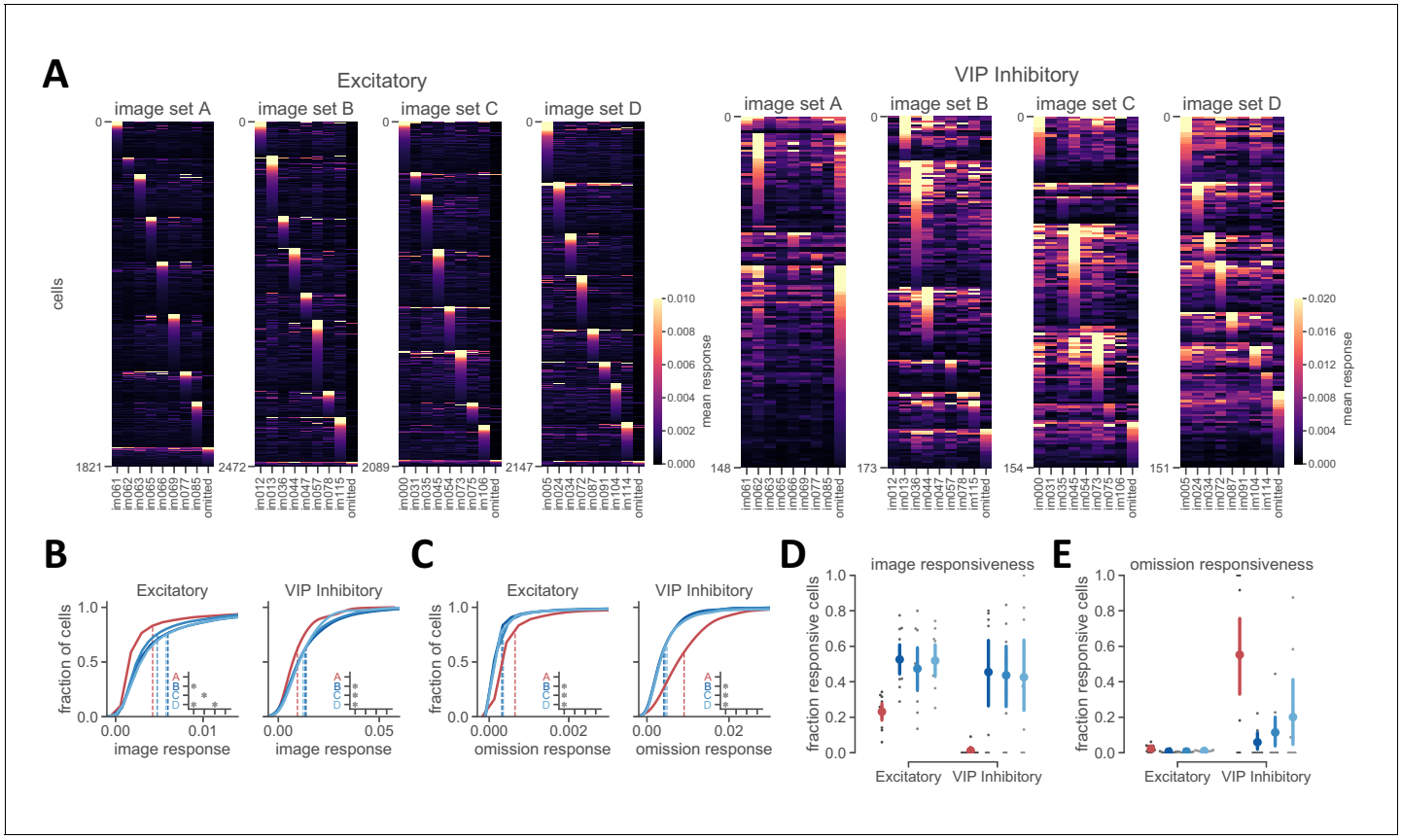

Figure 3. Reduced image-evoked activity for familiar stimuli. (**A**) Heatmap showing the mean response of excitatory (left panels) and VIP inhibitory (right panels) cells to images and stimulus omission for familiar and novel image sets. Response is computed using detected events in a 500 ms window after stimulus onset and averaged over all presentations of a given image or image omission. (**B**) Cumulative distribution of response magnitude for each cell's preferred image (excluding omissions) demonstrating reduced image-evoked activity for familiar compared to novel image sets. Insets show comparisons with p<0.008 (Welch's t-test with Bonferroni correction was used for all statistical comparisons, see Materials and methods for additional details). (**C**) Cumulative distribution of omission response magnitude across cells, demonstrating increased activity during stimulus omission for the familiar image set A. Insets are as described in panel **B**. (**D**) Fraction of image responsive cells is higher for novel image sets compared to the familiar image set. Image responsiveness is defined for each cell as having >25% of preferred image stimulus presentations with a significant response compared to a shuffled distribution of values taken from omission periods with extended gray screen. The fraction of image responsive cells is the number of cells within each session that meet the criterion for image responsiveness. Individual sessions are shown in gray, with mean across sessions ± 95% confidence intervals in color. p<0.008 for all comparisons with image set A. (**E**) Fraction of omission responsive cells is higher for the familiar image set in VIP inhibitory cells. Omission responsiveness is defined for each cell as having >10% of stimulus omissions with a significant response compared to a shuffled distribution of values taken from image presentations. The fraction of omission responsive cells is the number of cells within each session that meet the criterion for omission responsiveness. Individual sessions are shown in gray, with mean across sessions ± 95% confidence intervals in color. p<0.008 for A-B and A-C in VIP cells.

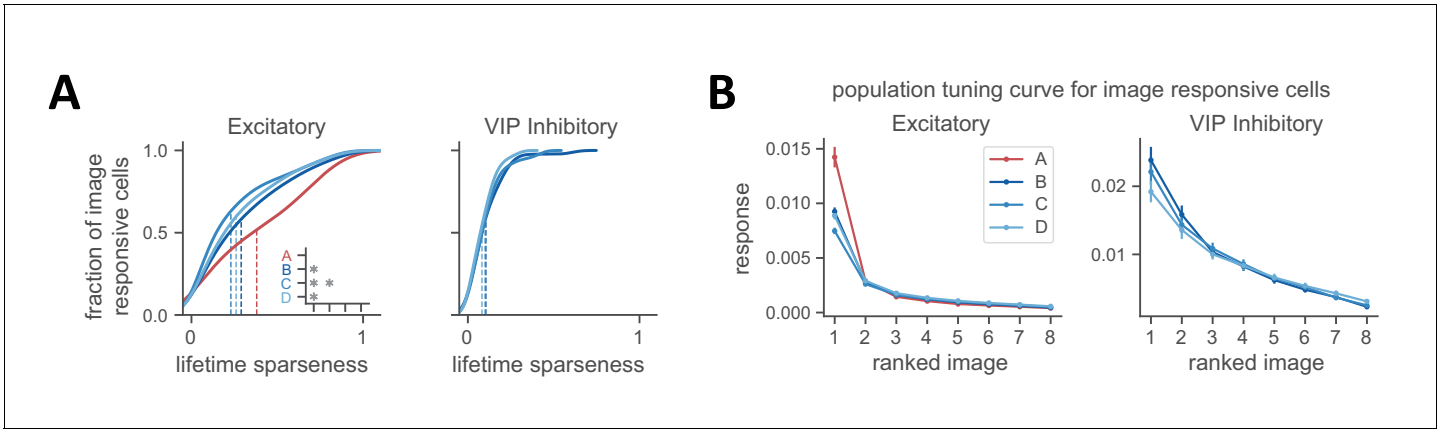

Figure 3—figure supplement 1. Response sparseness for familiar and novel images. (**A**) Cumulative distribution of lifetime sparseness values for cells meeting the criteria for image responsiveness described in ***Figure 3D***. Equation for lifetime sparseness is described in Materials and methods. Briefly, this value indicates whether a cell is highly selective in its response across images (value = 1), or whether it responds equally across images (value = 0). For excitatory cells, inset shows comparisons where $p<0.008$ (statistics described in Materials and methods). For VIP cells, no cells met the criteria for image responsiveness to the familiar image set A, and there were no significant differences across novel image sets. (**B**) Population tuning curves averaged across all cells meeting the criteria for image responsiveness. Each cell's response across images within an image set was rank sorted, then averaged. The excitatory population of image responsive cells shows an enhanced response to the preferred image. No image responsive cells for the familiar image set were present in the VIP inhibitory population, so no tuning curve for image set A is shown.

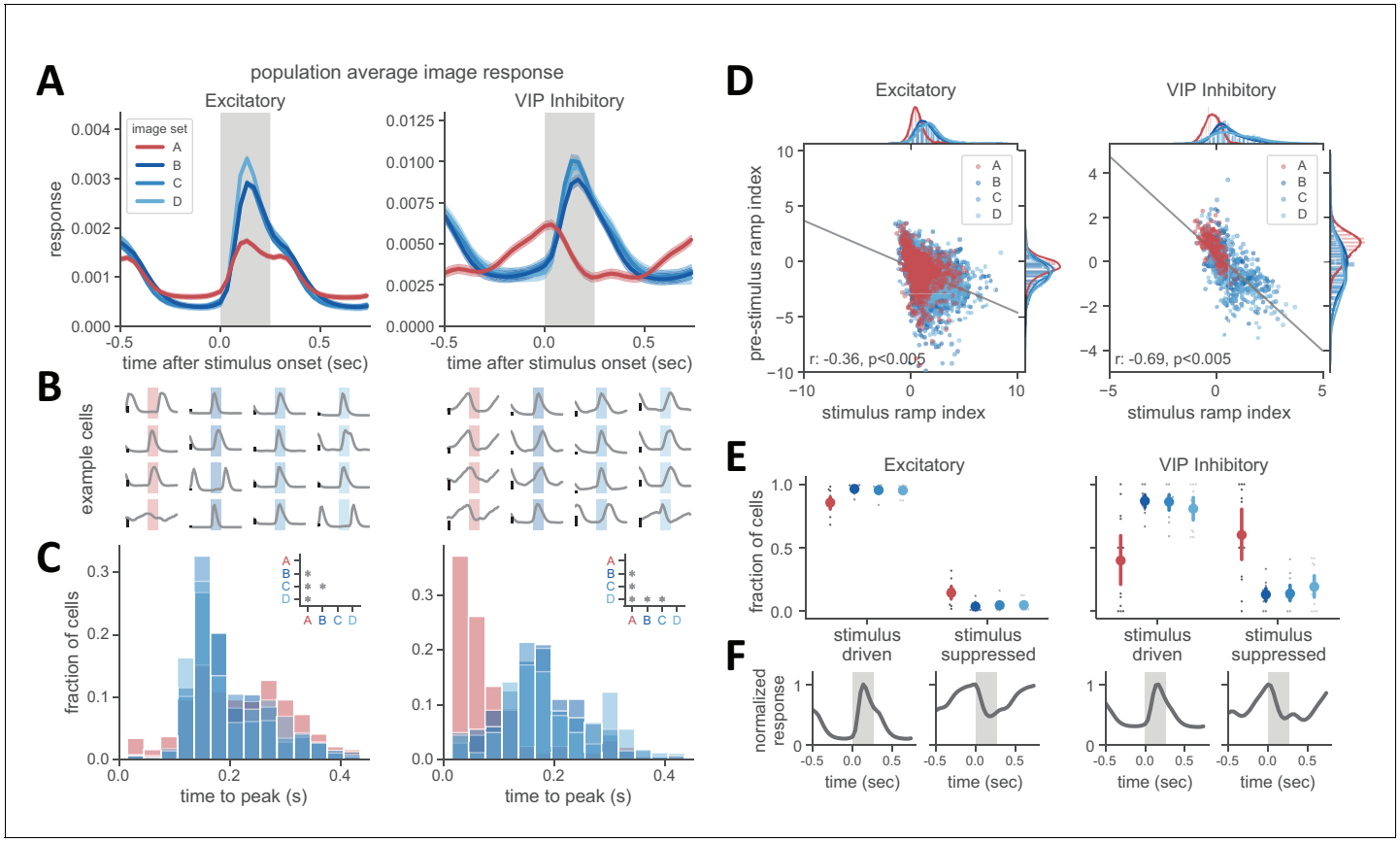

Figure 4. Experience-dependent shift in the dynamics of VIP inhibitory cells. (**A**) Population activity averaged over all image presentations for excitatory (left panel) and VIP inhibitory cells (right panel). Traces show mean ± SEM across cells. Note distinct dynamics in VIP population for novel versus familiar images sets. (**B**) Example single cell traces showing average image-evoked response for excitatory (left panel) and VIP inhibitory cells (right panel). Background shading denotes stimulus presentation, with color indicating the image set shown during the session for that cell. Each trace represents a unique cell recorded in a single session. Scale bar on left of each trace indicates a response magnitude of 0.005. (**C**) Histogram of time to peak response after stimulus onset for excitatory (left panel) and VIP inhibitory cells (right panel). Inset shows comparisons across image sets where $p<0.008$ (Welch's t-test with Bonferroni correction was used for all statistical comparisons, see Materials and methods for additional details). (**D**) Stimulus ramping and pre-stimulus ramping are negatively correlated. Each point is one neuron. The stimulus ramp index was computed over a 125 ms window after stimulus onset. The pre-stimulus ramp index was computed over a 400 ms window prior to stimulus onset. Data points across all image sets for each panel were fit with linear least-squares regression. Correlation and significance values for the fit are shown in lower left of each panel. (**E**) Novel image sets have an increased fraction of cells with stimulus-driven activity, whereas a larger fraction of cells was stimulus-suppressed for familiar images. Cells with a positive stimulus ramp index are considered stimulus-driven and those with a negative ramp index are stimulus-suppressed. $p<0.008$ for all comparisons with image set A. (**F**) Population average image evoked response for cells that met the criteria for stimulus driven or stimulus-suppressed, as described in panel **E**.

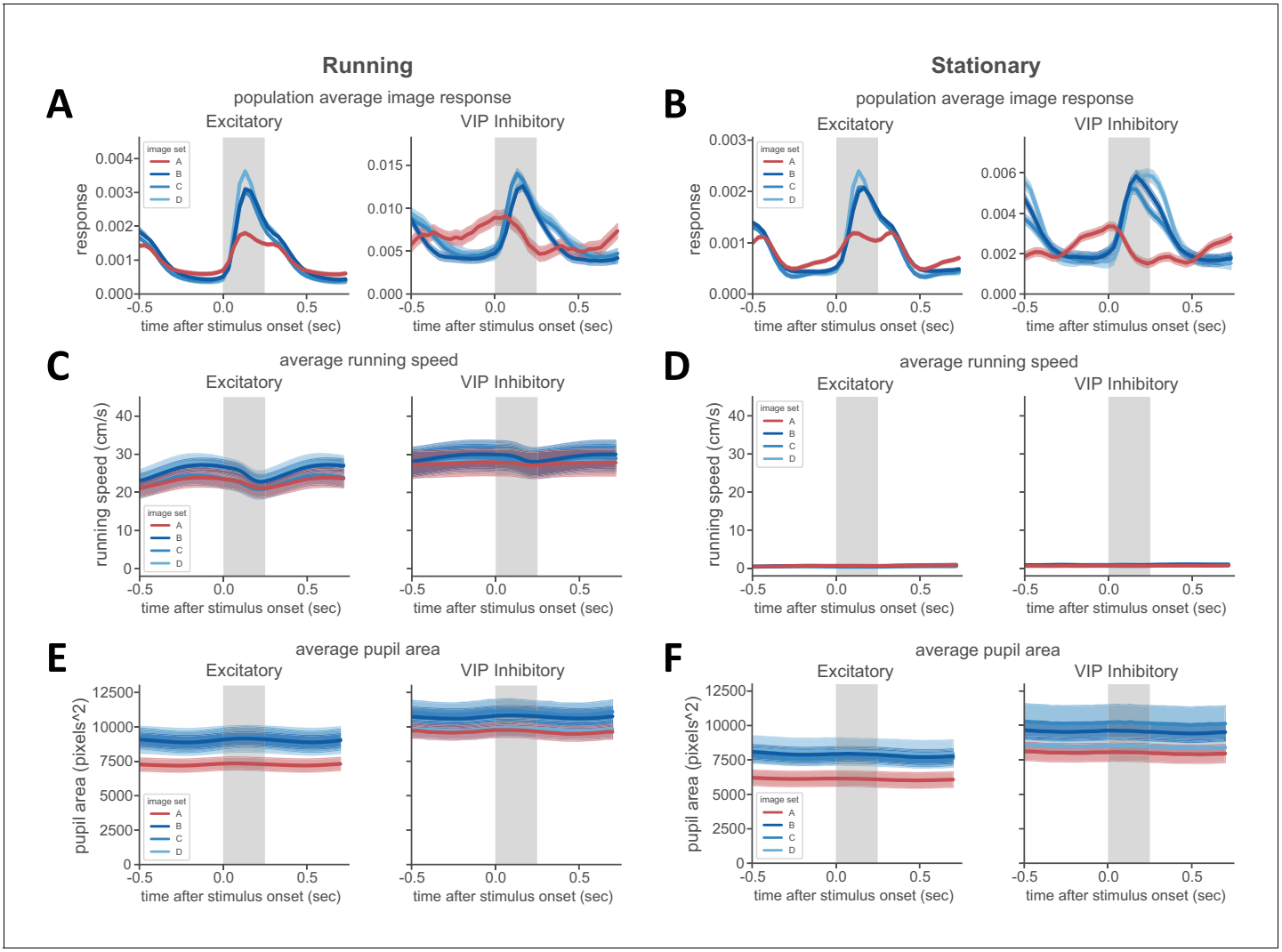

Figure 4—figure supplement 1. Changes in image-evoked VIP dynamics are not explained by running behavior or pupil diameter. (**A**) Average image-evoked response for excitatory (left panel) and VIP inhibitory cells (right panel) for image presentations where mice were running (mean running speed during the [−0.5, 0.75] second window around stimulus onset was greater than 5 cm/s). Mean image response during running was computed across all running image presentations for each cell, then averaged across cells. Traces show mean ± SEM across cells. (**B**) Averaged image-locked running speed for image presentations where mice were stationary (mean running speed during the [−0.5, 0.75] second window around stimulus onset was less than 5 cm/s). (**C**) Average stimulus-triggered running speed across image sets during image presentations where mice were running. Mean running speed was first calculated across all running image presentations within one session, then averaged across sessions. Traces show mean ± SEM across sessions. (**D**) Average stimulus-triggered running speed across image sets during image presentations where mice were stationary. (**E**) Average image-locked pupil area during image presentations where mice were running. Mean pupil area was first calculated across all running image presentations within a session, then averaged across sessions. Traces show mean ± SEM across sessions. (**F**) Average image-locked pupil area during image presentations where mice were stationary.

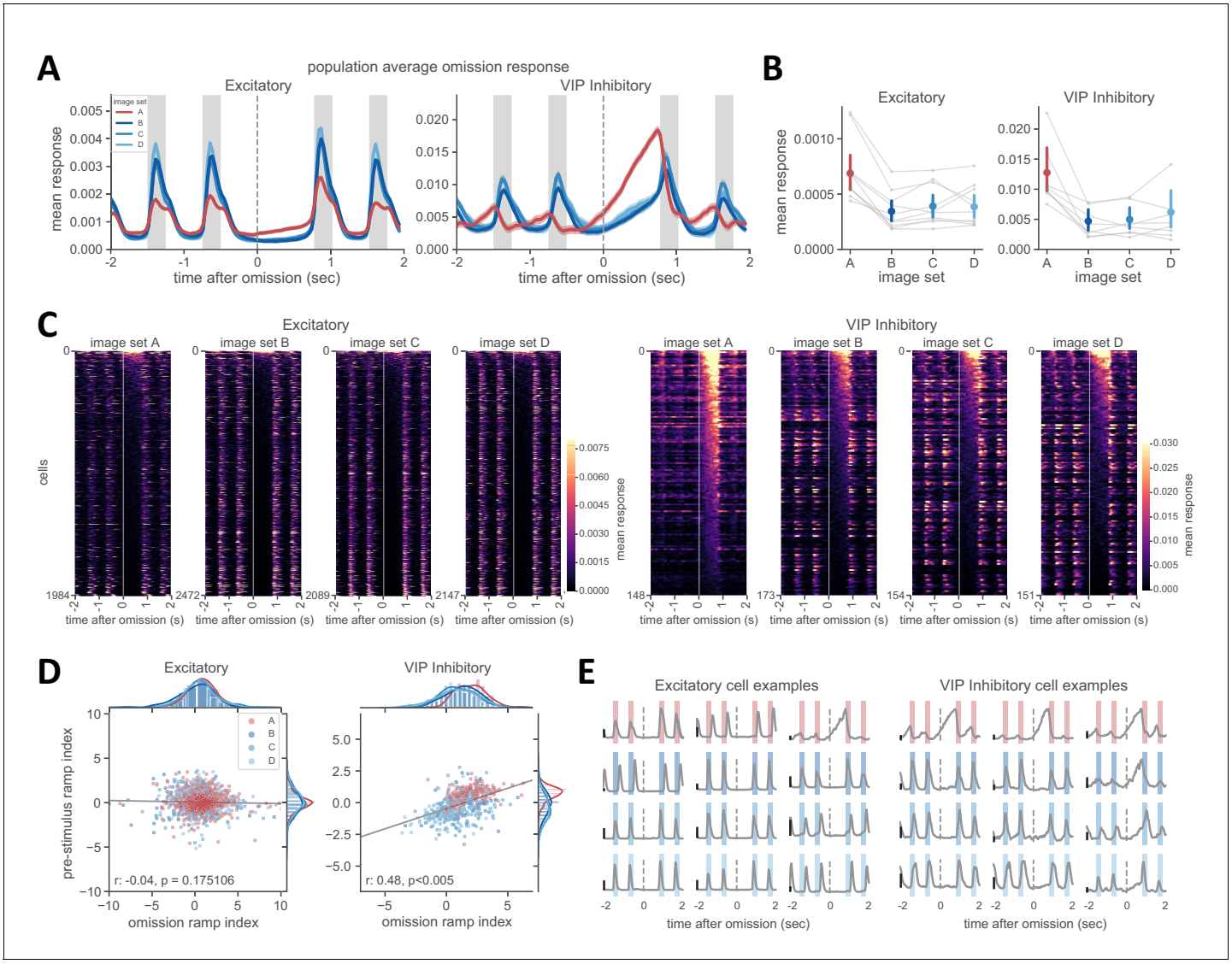

Figure 5. VIP cells show strong ramping activity during stimulus omission. (**A**) Average population activity around the time of stimulus omission. On average, excitatory neurons have little change in activity following stimulus omission (left panel). In contrast, activity of the VIP population for the familiar image set A continues to ramp up until the time of the next stimulus presentation. In sessions with novel images (image sets B, C, D), the VIP population also shows some change in activity following stimulus omission, but to a lesser degree than with familiar images. (**B**) Mean activity following stimulus omission is higher during sessions with the familiar image set A. The mean response in a 750 ms window following the time of stimulus omission was first computed for each cell in a given session, then averaged across cells in that session. Connected gray points indicate sessions recorded in a given mouse. Colored points represent the average across sessions for each image set ± 95% confidence intervals. $p<0.008$ for all comparisons with image set A, except A-C in VIP inhibitory cells (Welch's t-test used for all statistical comparisons, see Materials and methods for additional details). (**C**) Heatmap of activity around the time of stimulus omission across all excitatory (left panels) and VIP inhibitory cells (right panels), sorted by magnitude of activity in the omission window. Start of omission period is shown by white vertical line at time = 0 and extends to 750 ms thereafter when the next stimulus is presented. (**D**) The strength of the omission ramp index (y-axis) and pre-stimulus ramp index (x-axis) are positively correlated across VIP cells, but not excitatory cells, indicating that VIP cells with pre-stimulus activity typically also show ramping during stimulus omission. Data points across all image sets for each panel were fit with linear least-squares regression. Correlation and significance values for the fit are shown in lower left of each panel. (**E**) Example cells showing different response dynamics during stimulus (colored bars) and omission (time of expected stimulus indicated as gray dashed line) for excitatory and VIP inhibitory cells. Color of shaded bars indicates image set (familiar images in red, novel images in blue). Cells typically show either stimulus-evoked activity and no omission response, or pre-stimulus ramping and strong omission responses. Some cells (examples in right column of right panel) show a combination of stimulus-evoked and omission activity. Scale bar indicates a response of 0.01.

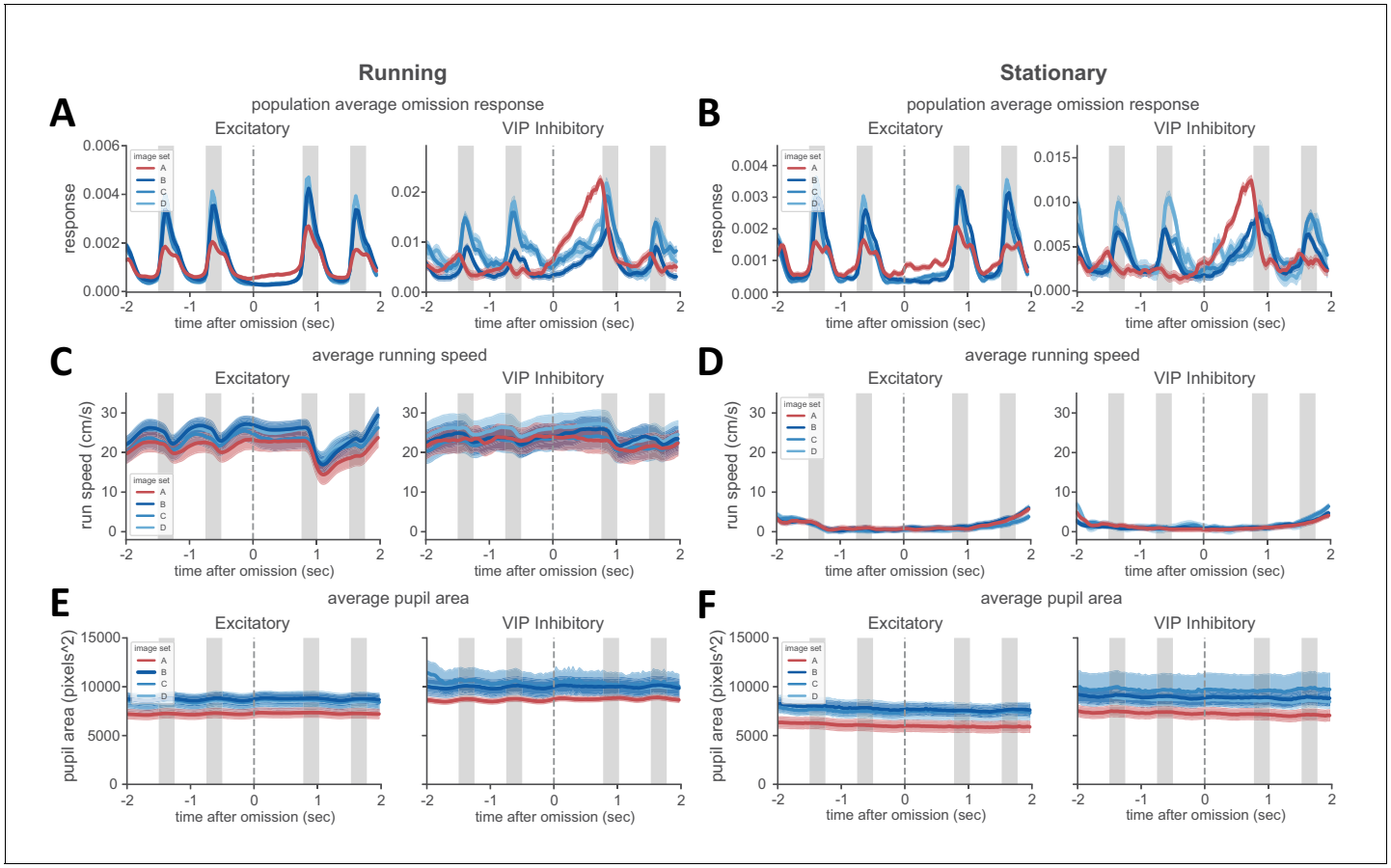

Figure 5—figure supplement 1. VIP omission ramping is not explained by running behavior or pupil diameter. (**A**) Average omission-triggered activity for excitatory (left panel) and VIP inhibitory cells (right panel) for omission trials where mice were running (mean running speed during the ± 2 s window around the omission time was greater than 5 cm/s). Traces show mean ± SEM across cells. (**B**) Averaged omission-triggered running speed for stimulus omissions where mice were stationary (mean running speed during the omission window was less than 5 cm/s). (**C**) Average omission triggered running speed across stimulus omissions where mice were running. Mean running speed was calculated for each session, then averaged across sessions. Traces show mean ± SEM across sessions. (**D**) Average omission-triggered running speed during stimulus omissions where mice were stationary. (**E**) Average omission-locked pupil area during stimulus omissions where mice were running. Mean pupil area was first calculated for each session, then averaged across sessions. Traces show mean ± SEM across sessions. (**F**) Average omission locked pupil area during stimulus omissions where mice were stationary.